JETIR.ORG ISSN: 2349-5162 | ESTD Year : 2014 | Monthly Issue
JOURNAL OF EMERGING TECHNOLOGIES AND INNOVATIVE RESEARCH (JETIR)
An International Scholarly Open Access, Peer-reviewed, Refereed Journal

Computational investigation of the solar air heater using a roughness V-shape rib

Sachin Baraskar[1], Santosh Kumar Rai[2]
[1]PhD scholar, [2]Research Director
[1]Department of Mechanical Engineering,
[1] Sri Satya Sai University of Technology and Medical Sciences, Sehore,
M.P., India-466001

Abstract : The current investigation involves a computational fluid dynamics (CFD) examination of a solar air heater that incorporates V-shaped ribs on the absorber plate along with artificial roughness. To analyze various fluid flow characteristics such as flow behavior, temperature distribution, and velocity distribution, the Renormalization group (RNG) k-e turbulent model is employed. A turbulence intensity of 5% is taken into account for exploring the aforementioned fluid flow properties, with consideration given to the relative roughness height (e/D) range spanning from 0.02 to 0.04, relative roughness pitch (P/e) set at 10, and an angle of attack (a) ranging from 30 to 90 degrees. The study encompasses working parameters including the Reynolds number (Re) ranging from 2000 to 20,000 and the intensity of solar radiations at 1000 W/m2. Monitoring of the direction and intensity of solar radiations is carried out using the Discrete Ordination (DO) model. The effective efficiency is theoretically analyzed for different relative roughness height values by applying the heat energy balance equation while maintaining the relative roughness pitch as a constant parameter. The findings reveal a maximum effective efficiency of 74% observed at Reynolds number and relative roughness height values of 14,000 and 0.034, respectively. This research contributes to the understanding of the performance of solar air heaters with V-shaped ribs and artificial roughness, providing valuable insights for enhancing energy efficiency in solar thermal systems. The utilization of advanced computational tools such as CFD and turbulence models offers a detailed investigation into the fluid dynamics within such systems, aiding in the optimization of their design and operation.

Keywords: Rib, Nusselt number, Reynolds number, heat transfer, efficiency

I. INTRODUCTION

The transfer of thermal energy between the absorber surface and the entering air within a traditional solar air heater is typically inefficient, resulting in a low thermal efficiency. This inefficiency leads to the formation of a laminar sub-layer near the absorber plate. To enhance its commercial viability, it is crucial to improve the thermal energy transfer coefficient by inducing turbulence in the heat transfer zone. Various methods can be employed to create turbulence in the heat transfer region, thereby boosting thermal efficiency. Among the different approaches, one effective method involves introducing roughness beneath the absorber plate to increase the heat transfer area and consequently enhance thermal efficiency. The simplest way to achieve this is by incorporating ribs or extended surfaces on the absorber plate [1-2].

Numerous studies have examined various forms of roughness geometries and their configurations. For instance, Parsad and Saini utilized short diameter wires in the transverse direction, while Gupta et al. emphasized the influence of rib proclivity, rib spacing (e/D), and Reynolds number when using angled ribs to control heat transfer[3-5]. Muluwork et al. investigated the impact of V-shaped discrete ribs on thermal energy transmission and fluid flow characteristics. Comparatively, Momin et al. observed a 2.30 times increase in the Nusselt number when V-shaped ribs were employed instead of smooth ducts. Karwa explored the effect of chamfered ribs on thermal energy transfer and noted that heat transfer initially increased with chamfer angle before reaching a plateau. Bhagoria et al. found that wedge-shaped ribs achieved maximum heat transfer at a 10-degree angle. Jaurker's research on grooved ribs revealed that optimal heat transfer occurred at a pitch-to-depth ratio of 6 and a groove location to pitch ratio of 0.4. Layek et al. conducted tests on chamfered rib grooves and demonstrated that a solar air heater with artificial roughness outperformed a smooth one [6-9].

In a similar vein, Bopche and Tandale employed U-shaped turbulators as roughness elements, noting a significant increase in heat transfer even at low Reynolds numbers [10]. Saini et al. [11] observed a sharp increase in the Nusselt number and friction factor when using arc-shaped ribs. Varun et al. conducted further research on enhancing thermal efficiency in solar air heaters through the manipulation of various roughness elements and geometries. Collectively, these studies underscore the importance of optimizing heat transfer through the strategic placement of roughness elements like ribs, grooves, and turbulators in solar air heaters, ultimately leading to improved thermal performance and efficiency in such systems. In their study, [12-14] conducted an investigation on a roughness element that featured transverse and inclined ribs. Their findings indicated that a value of (P/e) equal to 8 resulted in the optimal heat transfer performance. This research contributes to a deeper understanding of the behavior exhibited by such roughness elements and aids in predicting their performance under different conditions. Saini et al. [15] utilized dimple-shaped ribs as a form

of roughness element in their study, where they incorporated factors of friction and Nusselt number correlations. Yadav et al. [16–18] conducted research on the heat transfer performance of ribbed solar air heaters and noted that semicircular ribs exhibited the highest level of efficiency among different rib configurations. Several scholars have employed Computational Fluid Dynamics (CFD) to predict the performance of roughened solar air heaters [19–25]. Chaube et al. [26] specifically used CFD techniques to anticipate the performance of a solar air heater that had undergone artificial roughening. Saha et al. [27] applied Reynold's averaged Navier-Stokes procedure in their analysis to predict the heater's performance. Saini et al. [28] conducted performance analysis using CFD simulations focusing on arc-shaped ribs. Following a comprehensive investigation of various roughness geometries, it was observed that solar air heaters lacking roughness elements exhibit the lowest efficiency levels [29].
The current study focuses on the utilization of V-shaped ribs as roughness elements for conducting CFD analysis. Furthermore, the ribs have been strategically placed solely beneath the absorber plate to enhance heat transfer efficiency.

2. Duct details

The working and system variables utilized in the present study were carefully selected in accordance with the guidelines outlined in ASHARE 93-77 [30]. Among the various components of the solar air heater, the duct emerged as the most crucial element. It is noteworthy that the inner cross-sectional area of the duct, as illustrated in Figure 1, was precisely assessed for the purpose of this analytical investigation and was found to be 200 mm x 20 mm. The adherence to the recommendations provided by ASHARE 93-77 [30] ensured that the chosen working and system variables were appropriate for the study's objectives. The meticulous consideration given to the duct's characteristics underscores the significance of this component in the overall performance of the solar air heater. The detailed evaluation of the duct's inner cross-sectional area further enhances the validity and reliability of the study's findings, thereby contributing to the advancement of knowledge in the field of solar energy utilization.

3. NUMERICAL MODEL

3.1. Details of the geometry

Ribs in a V-shaped configuration located beneath the absorber plate have been utilized as a form of surface roughness. The computational fluid dynamics (CFD) analysis included the generation of the solution domain, as depicted in Figure 1. A duct with dimensions of (1530 x 210 x 15 mm) was the subject of examination. The absorber plate had a thickness of 0.5 mm. While the bottom and top of the duct were ribbed, the other three surfaces remained smooth.

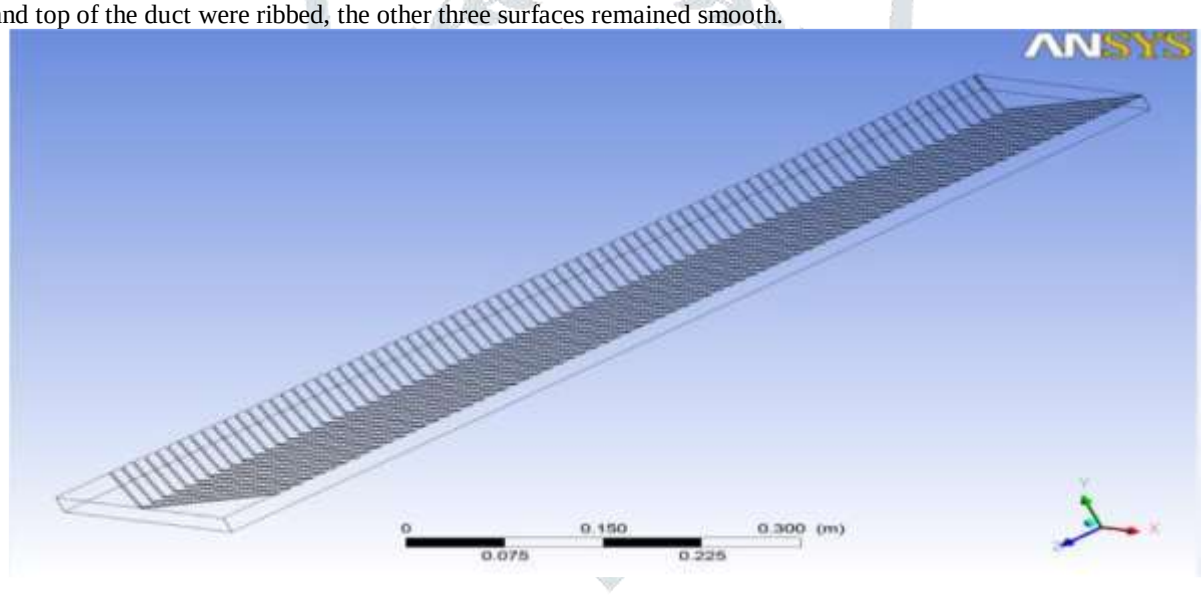

Fig. 1. Arrangement of ribs on the inner side of absorber.

3.2. Grid

Rather than employing a two-dimensional model for analyzing flow characteristics and heat transfer, a three-dimensional model has been developed due to the occurrence of secondary flows. Tetrahedral (Patch independent) meshing was utilized to achieve higher accuracy in the results, as illustrated in Figure 2. The model consisted of 94564 nodes and 378966 elements.

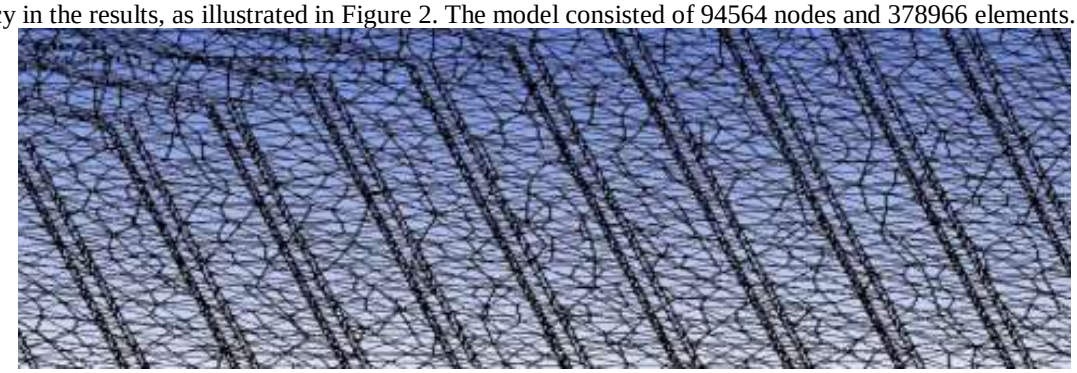

Fig. 2. Mesh detail (V shaped ribs).

3.3. Computational investigation

For the purpose of this research, the ANSYS workbench software was utilized for fluid flow simulations. The ANSYS workbench is capable of accurately determining parameters such as temperature at the exit, velocity, and flow behavior due to the application of thermal loading. In this investigation, several assumptions were considered. Firstly, the working medium was assumed to be air, displaying ideal gas characteristics. Secondly, the flow was assumed to be steady, three-dimensional, and turbulent in nature. Thirdly, it was assumed that the system is well-insulated, preventing any heat loss to the surrounding atmosphere. Furthermore, it was assumed that the thermal conductivity of the wall and ribs material remains constant regardless of temperature variations. Additionally, the materials were assumed to be homogeneous and isotropic in their properties. The inlet boundary condition, determined using Reynold's number, was specified as velocity, while the outlet boundary condition was set as outflow.

3.4. Description of V shape rib duct

The copper wire arranged in ribs (V-shaped) was responsible for the roughness present on the underside of the plate which facilitated the absorption of solar radiation. The absorber plate, constructed from aluminum, incorporated ribs in a V-shaped pattern with an angle of 60 degrees. The range of Reynold's number taken into account for this study spanned from 2000 to 20000, a range typically encountered in the operation of solar air heaters. This parameter is crucial for determining the flow behavior and heat transfer characteristics within the system.

4. RESULTS ANALYSIS

4.1. Model selection

For the selection of validating a model air heater that is analogous in dimensions to a roughened solar air heater, various models have been examined. These include the Realizable k- ε model, the Renormalization Group (RG) model, the Standard k- ε model, and the Shear Stress Transport (SST) model. Subsequently, the outcomes were compared with the correlations provided for a smooth solar air heater as indicated by Dittus-Bolter [31]. The relationship

$$Nu = 0.024Re^{0.8}Pr^{0.4} \quad \ldots\ldots(1)$$

Was utilized, where Pr represents the Prandtl Number. Upon analysis, it was observed in Figure 4 that the results obtained using the Renormalization group k- ε model exhibit only slight differences in comparison to those acquired through the correlation supplied by Dittus-Bolter for the smooth solar air heater. This comparison sheds light on the effectiveness and accuracy of the models employed in predicting the behavior of the air heater systems. Additional research and experimentation may be necessary to further validate and refine these models for enhanced predictive capabilities in future applications.

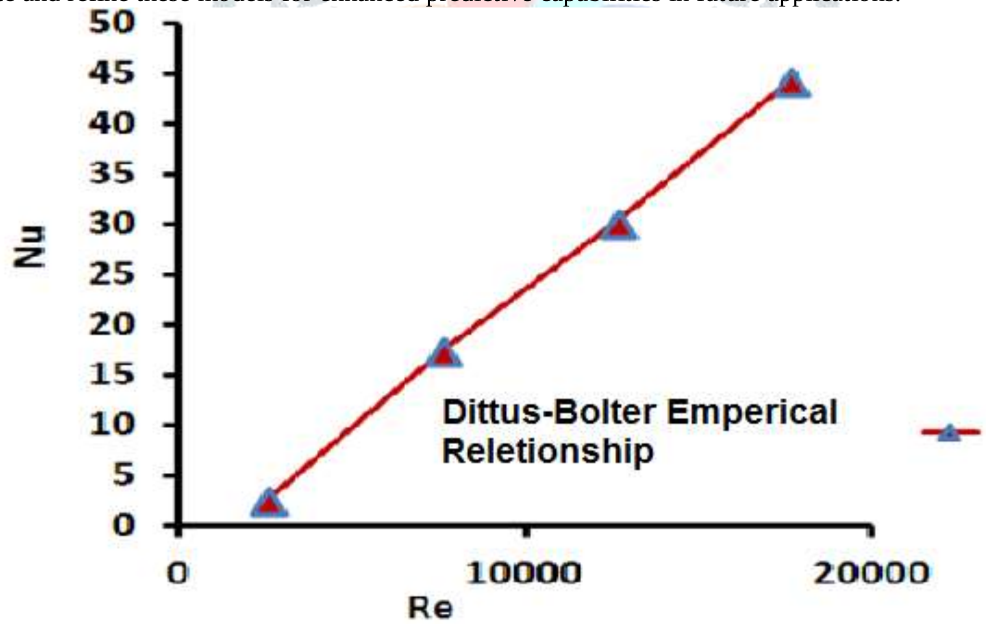

Fig. 3. Variation of Nusselt number with Reynold's number for different model (a) Dittus-Bolter Emperical Reletionship

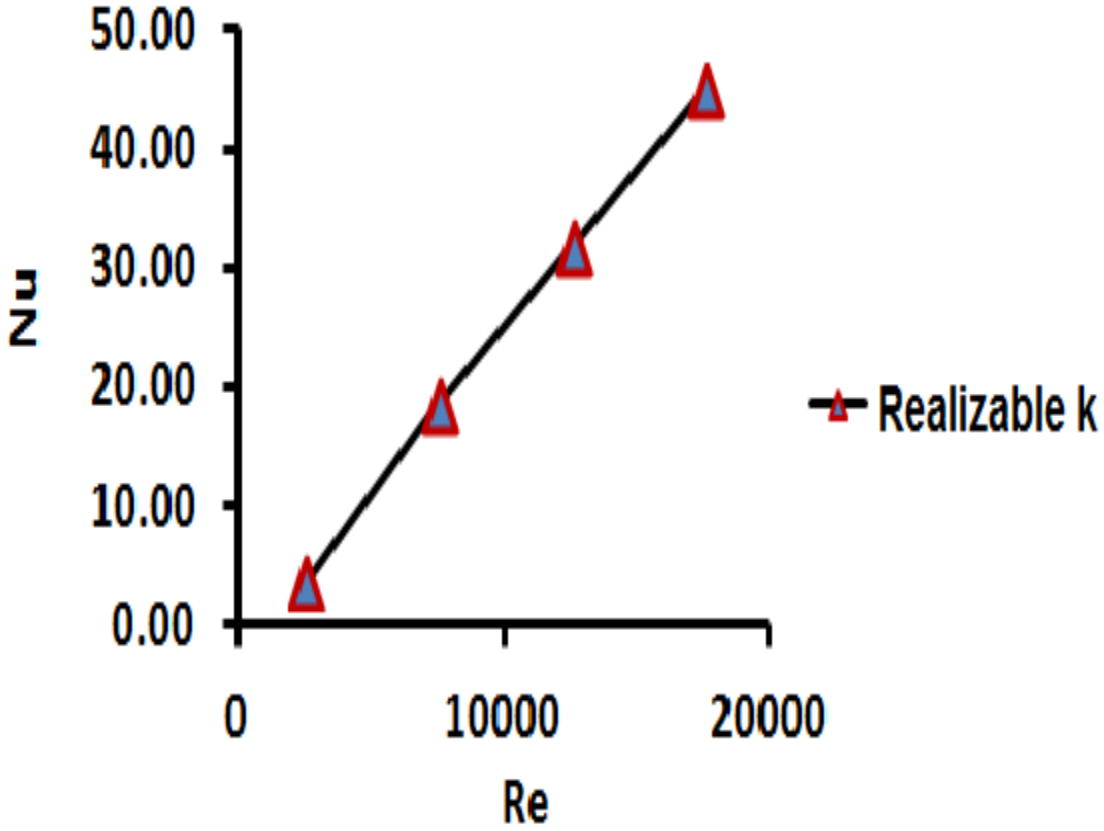

Fig. 3. Variation of Nusselt number with Reynold's number for different model (b) Realizable k

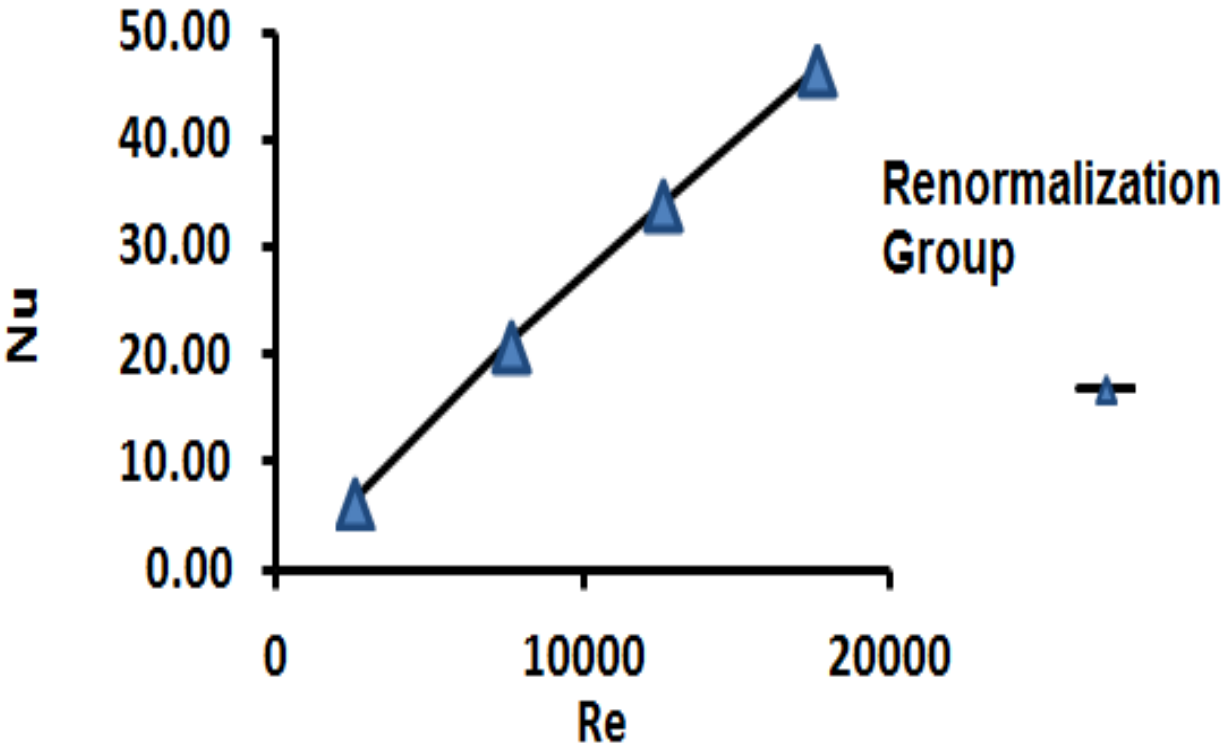

Fig. 3. Variation of Nusselt number with Reynold's number for different model (c) Renormalization Group

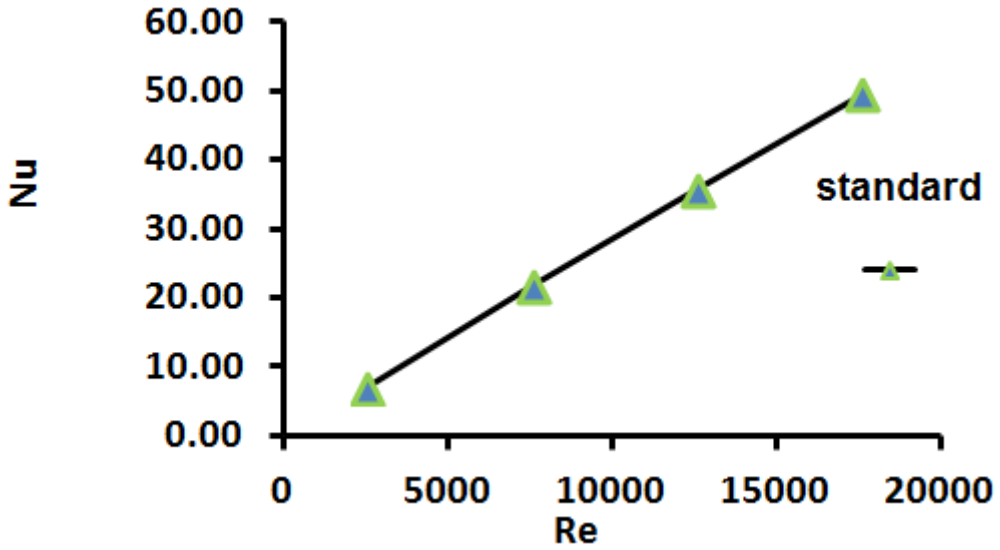

Fig. 3. Variation of Nusselt number with Reynold's number for different model (d) standard

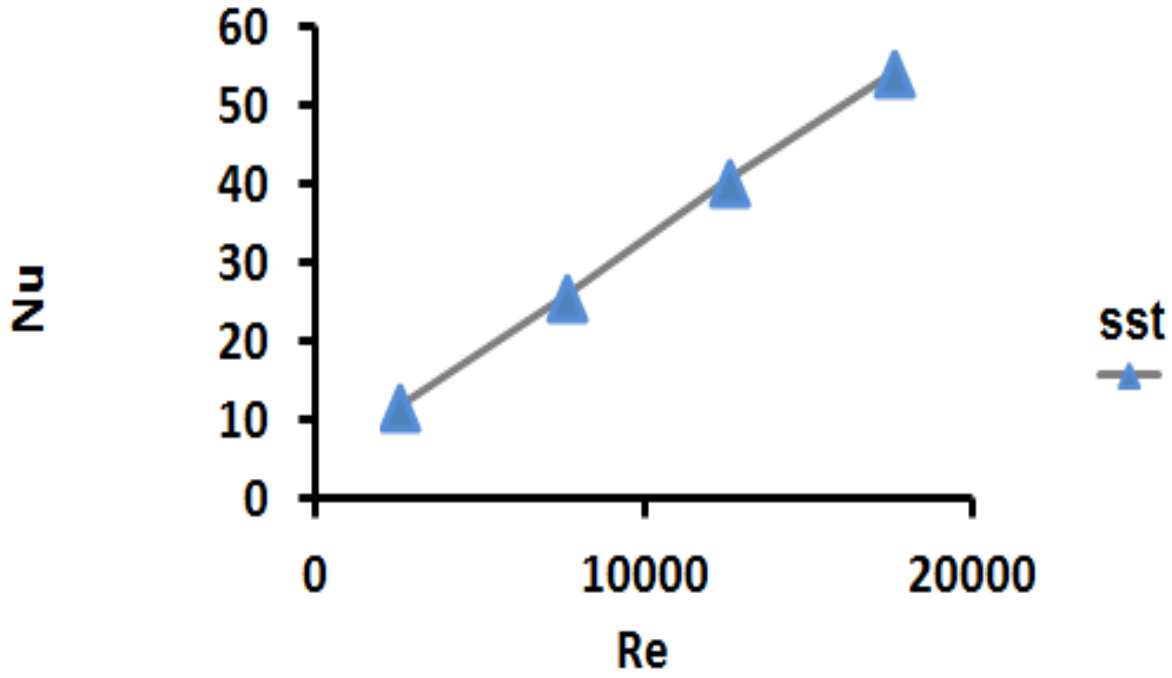

Fig. 3. Variation of Nusselt number with Reynold's number for different model (e) sst

in this study, the Nusselt number is analyzed in relation to Reynold's number across various models, showcasing a detailed comparison. The investigation displayed the highest level of disparity in results when examining the empirical correlation for a smooth duct, firstly with the Shear Stress Transport model and subsequently with the Standard k- ε model. Additionally, the Realizable model exhibited a significant level of deviation in its findings. Therefore, in order
to address these discrepancies, the Renormalization group ke model has been implemented in the current research. This choice was made to ensure a more accurate and reliable analysis of the Nusselt number in relation to Reynold's number within the context of different models. The utilization of the Renormalization group k- ε model is expected to provide more precise results and enhance the overall understanding of heat transfer characteristics in duct systems.

4.2. Simulation results

The presence of ribs has a significant impact on both the thermal transmission and fluid dynamic parameters of flow. The Nusselt number is clearly demonstrated in Figure 4. The V-shaped ribs lead to the separation of the fluid layer from the wall, resulting in a reduction in heat transfer along the downstream of the rib. However, simultaneously, the vortices effect that is created just downstream of the rib promotes fluid mixing, leading to higher heat transfer rates. Moreover, in the vicinity of the downstream of the rib along the direction of flow, the vortices effect tends to dominate the boundary layer separation, thereby further enhancing heat transfer. The computational fluid dynamics (CFD) analysis conducted has meticulously examined the flow separation and reattachment, providing valuable insights into other related phenomena. This detailed analysis aids in elucidating the complex interactions between the ribbed surfaces and the flow characteristics, contributing to a deeper understanding of the heat transfer mechanisms involved. It is evident that the presence of ribs alters the flow behavior significantly, leading to intricate fluid dynamics that play a crucial role in determining the overall heat transfer efficiency. The findings from these studies can be applied to optimize the design of heat exchangers and other thermal systems for enhanced performance and efficiency. Additionally, the insights gained

from such research can potentially inform the development of more effective heat transfer enhancement techniques in various engineering applications.

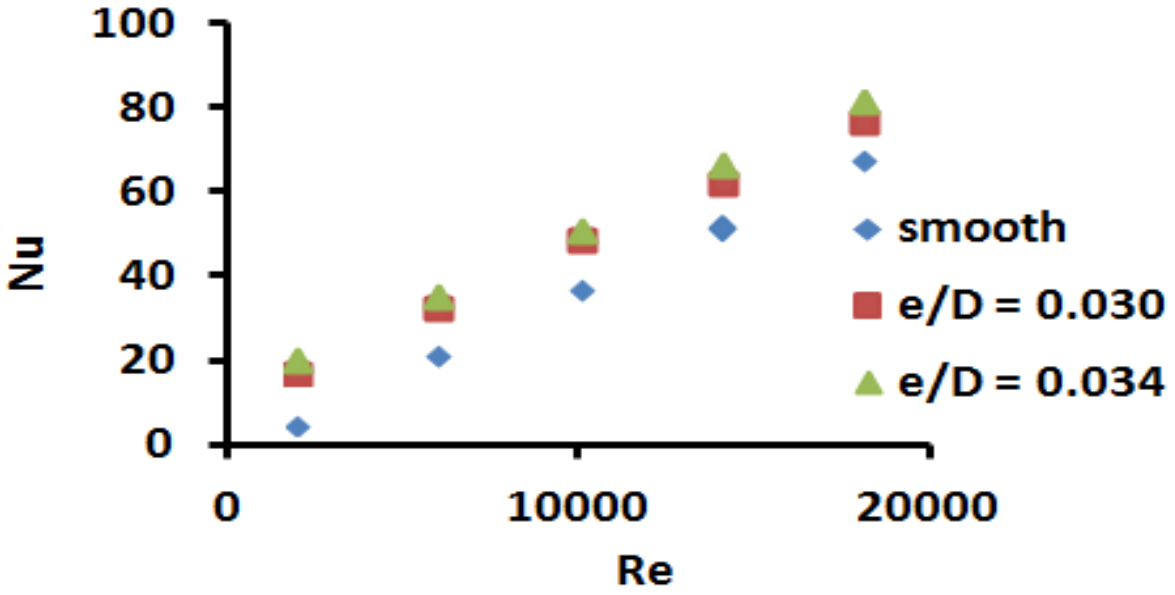

Figure 4: Variation of Nu vs. Re

4.3. Roughness height upshot on Nusselt No.

Figure 5 illustrates the correlation between Nusselt Number and Reynolds Number for different (e/D) ratios, all the while upholding the relationship.

The constant value is maintained at 1.0. For all values of the ratio of the diameter to the characteristic length, the Nusselt Number shows an upward trend with an increase in Reynolds Number, suggesting a rise in the rate of heat transfer. Specifically, as the ratio of the diameter to the characteristic length increases from 0.030 to 0.034, the Nusselt Number also experiences a corresponding increase.

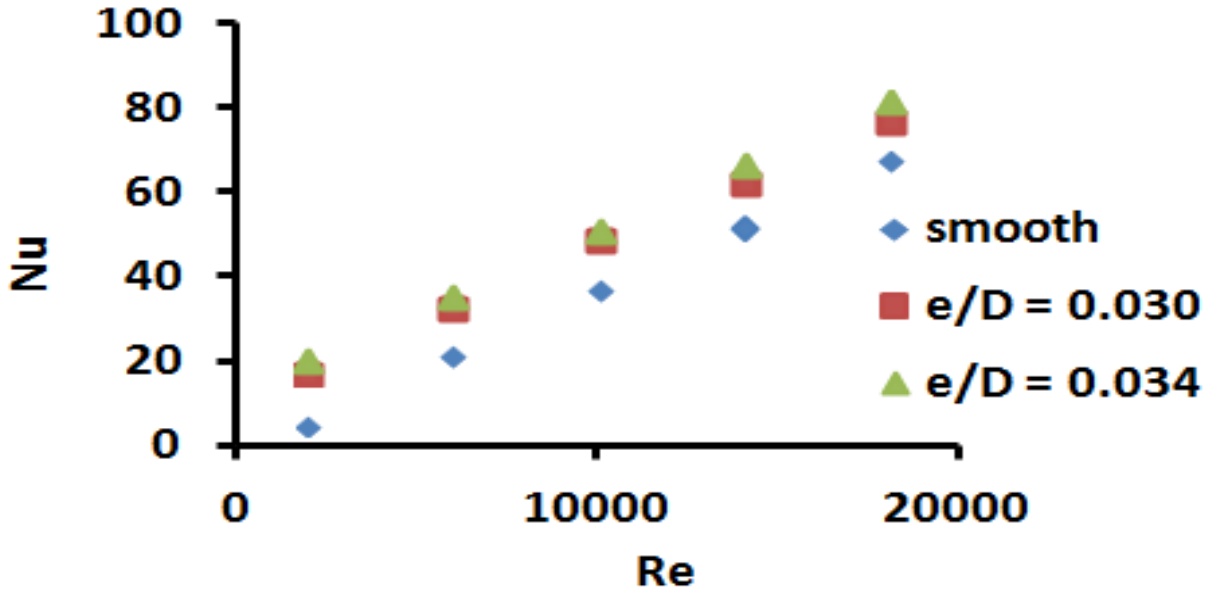

Fig.5. Nusselt number vs Reynold's number at different values of (e/D).

4.4. Nusselt No. Variation with arc angle

Fig. 6 illustrates the variation in Nusselt Number disparity with Reynold's Number for different values of (a/60) while maintaining the constant value of (e/D) at 0.034. The Nusselt number increases as the Reynold's number increases across all values of (a/60). However, when the value of (a/60) is raised from 0.50 to 0.66 while keeping the values of (e/D) and Reynold's number constant, the Nusselt number decreases.

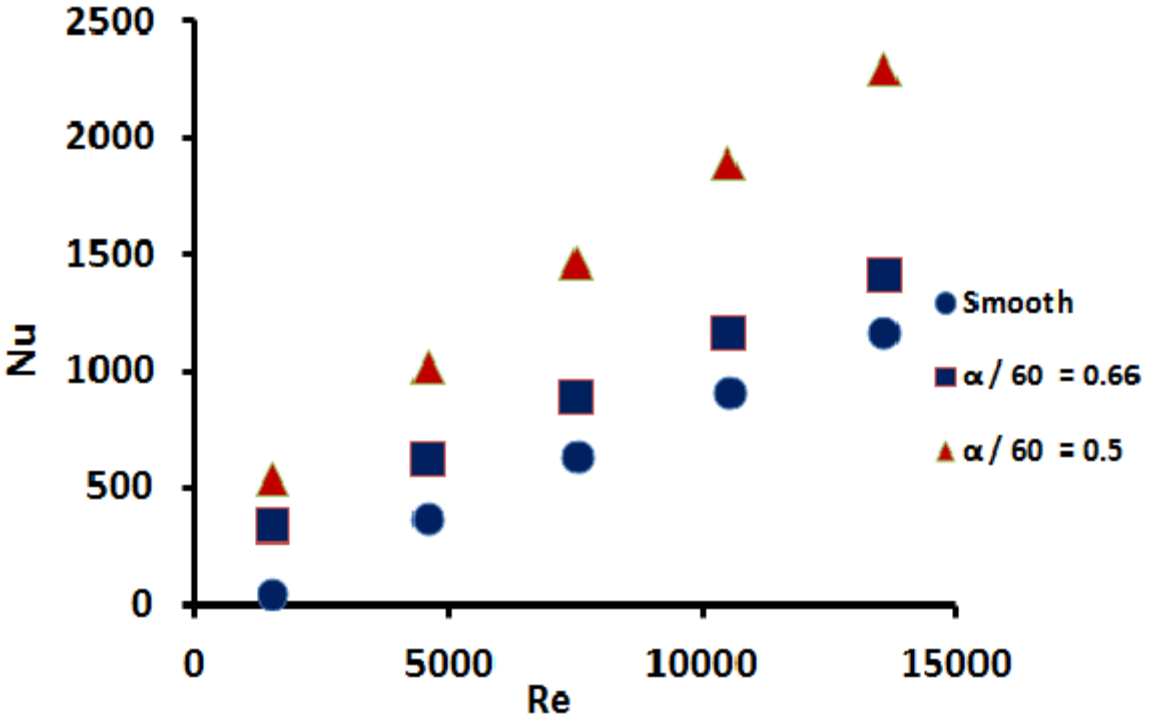

Fig. 6. Nusselt no. vs Reynold's no. at various value of (a/60).

4.5. Friction factor variation with height of roughness element

Figure 7 depicts the relationship between the friction factor and Reynold's number for various (e/D) values at a consistent (a/60) value of 1.0. As the Reynold's number increases, the friction factor decreases. Conversely, the friction factor rises as the (e/D) value increases from 0.030 to 0.034 under specific flow conditions.

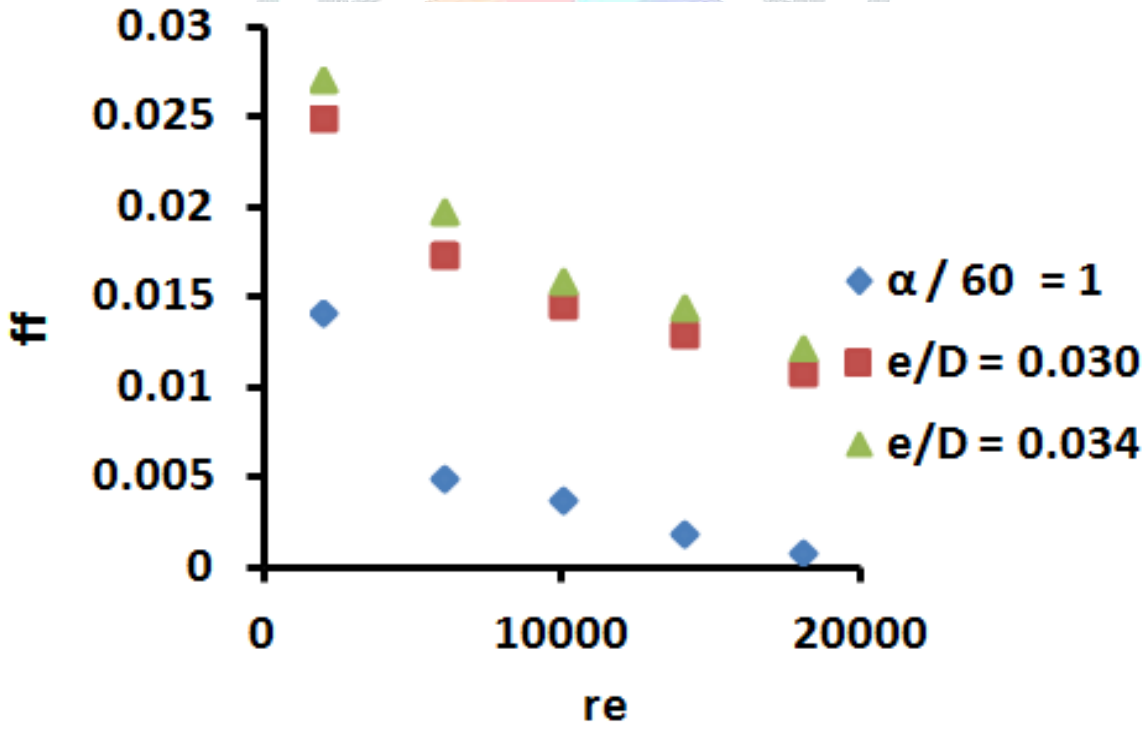

Fig. 7. Friction factor variation with Reynold's number at different values of (e/D).

4.6. Upshot of relative arc angle on friction factor (f)

Fig. 8 illustrates the variation in the friction factor (f) as a function of Reynolds number for different values of (a/60), with the ratio (e/D) held constant at 0.034. The findings indicate that an increase in the (a/60) ratio from 0.50 to 0.66 leads to a rise in the friction factor. These outcomes display a trend that has been previously observed by various researchers in their experimental investigations.

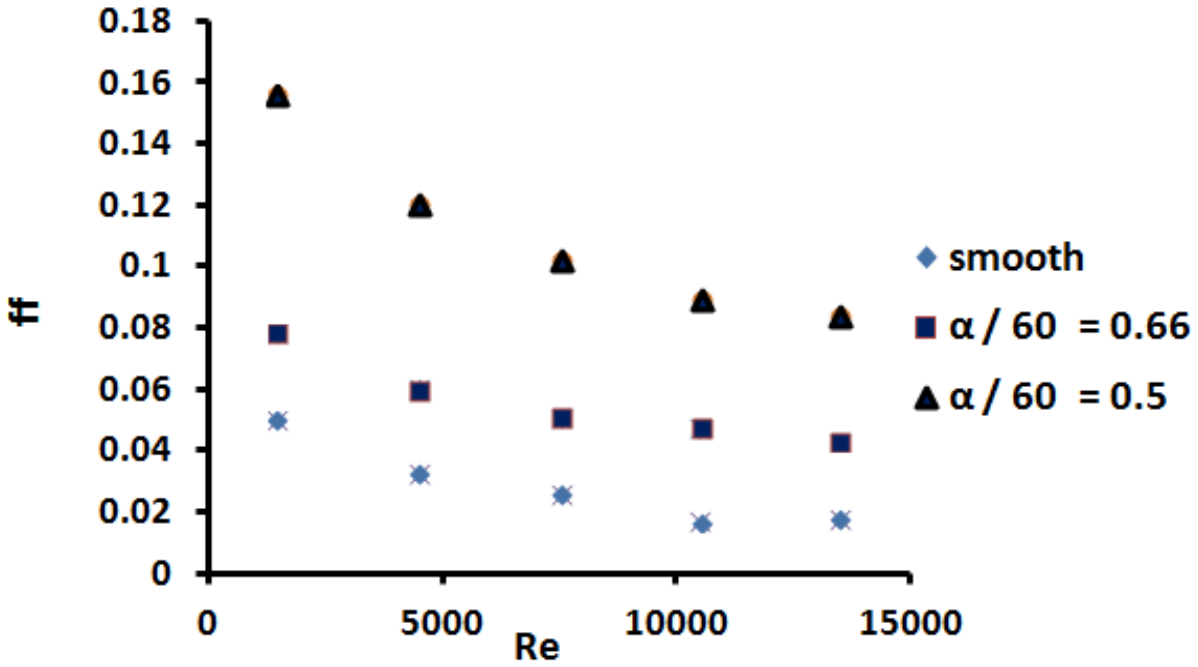

Fig. 8. Friction factor (f) vs Reynolds no. at different value of (a/60).

4.7. Effective efficiency

The presence of roughness on the absorber's surface enhances the thermal efficiency of an air heater, despite this, there are some drawbacks. a substantial increase in the power required for pumping is essential due to the necessity of applying more force to push air into the duct of a solar air heater through increased pump work. Consequently, the selection of roughness geometry must be made based on characteristics that consider both thermal and hydraulic performance aspects. The calculation of effective efficiency involves subtracting the thermal energy needed to overcome frictional power from the usable energy gain of the collector, as proposed by Cortes and Piacentini [32]. The formula for determining effective efficiency is expressed as the quotient of useful energy gained by the incident solar radiation. The graph displayed in Fig. 11 illustrates how the effective efficiency of an air heater with ribs on its absorber surface, acting as a roughness element, changes with Reynolds' number. It is observed that for all (e/D) ratios, the effective efficiency increases with Reynolds' number and reaches a peak value before decreasing, as depicted in Fig. 9. This trend may be attributed to the influence of mechanical power on the system. In the current investigation, the value of (P/e) remains constant at 10 for all (e/D) ratios. Lower Reynolds numbers exhibit enhanced effective efficiency with larger (e/D) ratios, whereas higher Reynolds numbers show improved efficiency with smaller (e/D) ratios. Furthermore, it was established that an effective efficiency of approximately 74 percent is achieved at a Reynolds number of 14000 when the (P/e) ratio is 0.034. The study indicates that the influence of Reynolds' number and roughness characteristics plays a significant role in the performance of the solar air heater system. The findings suggest that optimizing the roughness geometry can lead to the enhancement of thermal and hydraulic efficiencies in solar air heating applications. Future research could explore the impact of different roughness elements and Reynolds numbers on the overall efficiency and performance of solar air heaters, providing valuable insights for design and optimization processes in renewable energy systems.

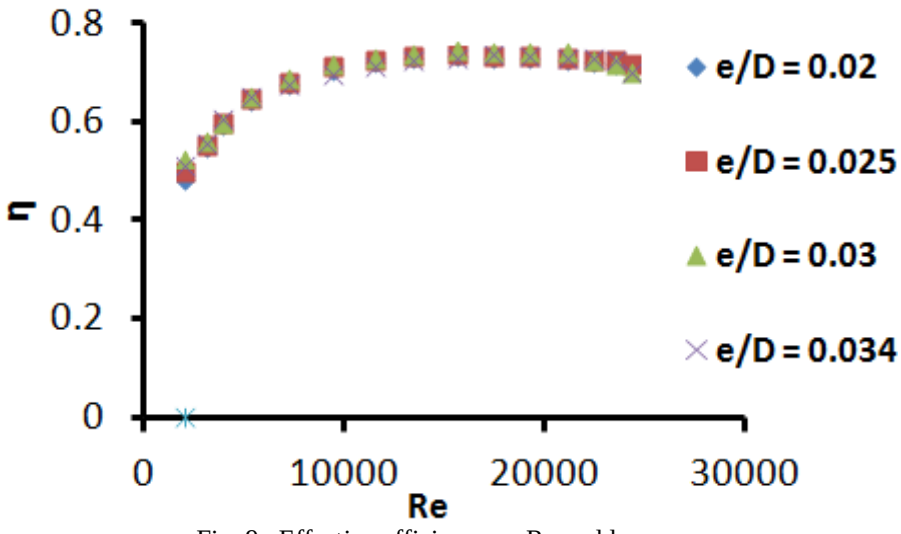

Fig. 9 . Effective efficiency vs Reynolds no

5. Conclusions

To predict the dynamic fluid characteristics with precision, a computational fluid dynamics (CFD) analysis was carried out on an air heater featuring roughness on its absorber surface in the form of V-shaped ribs. Numerous CFD models were scrutinized in comparison to the empirical correlation established by Dittus Bolter for a smooth duct to ensure validation. The results derived from the Renormalization group ke model displayed a high level of agreement with the analytical solution. The Nusselt number exhibits

fluctuations in accordance with the Reynold's number for a specific value of e/D, and it experiences an increase as the relative roughness height escalates for all Reynold's number values when the ratio of a/60 remains constant. Correspondingly, the Nusselt number demonstrates a similar trend to the Reynold's number for all a/60 values at a fixed e/D value. Nevertheless, the Nusselt number diminishes as the a/60 ratio rises, and this deviation becomes more pronounced at elevated Reynold's number values. In contrast, the friction factor decreases with Reynold's number for all e/D values while maintaining a constant a/60 ratio. Notably, it was established that with a consistent e/D value of 0.034, the friction factor declines as the a/60 ratio increases. Moreover, for an e/D value of 0.034, the effective efficiency surges by up to 74 percent at a Reynold's number of 14000.

REFERENCES

[1] B.N. Prasad, J.S. Saini, Effect of artificial roughness on heat transfer and friction factor in a solar air heater, Solar energy 41 (6) (1988) 555–560.

[2] D. Gupta, S.C. Solanki, J.S. Saini, Thermohydraulic performance of solar airheaters with roughened absorber plates, Solar energy 61 (1) (1997) 33–42.

[3] D. Gupta, S.C. Solanki, J.S. Saini, Heat and fluid flow in rectangular solar air heater ducts having transverse rib roughness on absorber plates, Solar energy 51 (1) (1993) 31 37.

[4] Muluwork, K., Investigations on fluid flow and heat transfer in roughened absorber solar heaters. India: IIT, Roorkee-247667, 2000.

[5] A.-M. Ebrahim Momin, J.S. Saini, S.C. Solanki, Heat transfer and friction in solar air heater duct with V-shaped rib roughness on absorber plate, Int. J. Heat Mass Transfer 45 (16) (2002) 3383–3396.

[6] R. Karwa, S. Solanki, J. Saini, Thermo-hydraulic performance of solar air heaters having integral chamfered rib roughness on absorber plates, Energy 26 (2) (2001) 161–176.

[7] J.L. Bhagoria, J.S. Saini, S.C. Solanki, Heat transfer coefficient and friction factor correlations for rectangular solar air heater duct having transverse wedge shaped rib roughness on the absorber plate, Renew. Energy 25 (3) (2002) 341– 369.

[8] A.R. Jaurker, J.S. Saini, B.K. Gandhi, Heat transfer and friction characteristics of rectangular solar air heater duct using rib-grooved artificial roughness, Solar Energy 80 (8) (2006) 895–907.

[9] A. Layek, J.S. Saini, S.C. Solanki, Effect of chamfering on heat transfer and friction characteristics of solar air heater having absorber plate roughened with compound turbulators, Renew. Energy 34 (5) (2009) 1292–1298.

[10] A. Layek, J.S. Saini, S.C. Solanki, Heat transfer and friction characteristics for artificially roughened ducts with compound turbulators, Int. J. Heat Mass Transfer 50 (23-24) (2007) 4845–4854.

[11] S.B. Bopche, M.S. Tandale, Experimental investigations on heat transfer and frictional characteristics of a turbulator roughened solar air heater duct, Int. J. Heat Mass Transfer 52 (11-12) (2009) 2834–2848.

[12] S.K. Saini, R.P. Saini, Development of correlations for Nusselt number and friction factor for solar air heater with roughened duct having arc-shaped wire as artificial roughness, Solar Energy 82 (12) (2008) 1118–1130.

[13] R. Saini, S. Singal, Investigation of thermal performance of solar air heater having roughness elements as a combination of inclined and transverse ribs on the absorber plate, Renew. Energy 33 (6) (2008) 1398–1405.

[14] A. Patnaik, R. Saini, S. Singal, Performance prediction of solar air heater having roughened duct provided with transverse and inclined ribs as artificial roughness, Renew. Energy 34 (12) (2009) 2914–2922.

[15] R.P. Saini, J. Verma, Heat transfer and friction factor correlations for a duct having dimple-shape artificial roughness for solar air heaters, Energy 33 (8) (2008) 1277–1287

[16] A.S. Yadav, O.P. Shukla, A. Sharma, I.A. Khan, CFD analysis of heat transfer performance of ribbed solar air heater, Mater. Today Proc. (2022),

[17] A.S. Yadav et al., Numerical simulation and CFD-based correlations for artificially roughened solar air heater, Mater. Today Proc. 47 (2021) 2685– 2693.

[18] A.S. Yadav, M.K. Dwivedi, A. Sharma, V.K. Chouksey, CFD based heat transfer correlation for ribbed solar air heater, Mater. Today Proc. (2022),

[19] A.S. Yadav, J.L. Bhagoria, A CFD based thermo-hydraulic performance analysis of an artificially roughened solar air heater having equilateral triangular sectioned rib roughness on the absorber plate, Int. J. Heat Mass Transfer 70 (2014) 1016–1039.

[20] Navneet, Arya., Varun, Goel. (2023). Comparative study of V-ribs miniature with dimple hybrid roughness along with dimples shaped roughness used in solar air heating system. Energy Sources Part A-recovery Utilization and Environmental Effects, doi: 10.1080/15567036.2023.2195822

[21] S. Khamitkar, D.O. Hebbal, Performance Analysis of Solar Air Heater Using CFD, Int. J. Eng. Res. Technol. 8 (2013) 1771–1776.

[22] S.V. Karmare, A.N. Tikekar, Analysis of fluid flow and heat transfer in a rib grit roughened surface solar air heater using CFD, Solar Energy 84 (3) (2010) 409– 417

[23] Akash, Dwivedi., Mohammad, Mohsin, Khan., Abhijit, Dey., Mohammad, Irfan, Hajam. (2023). Computational Analysis of the Effect of Flow Parameters on Friction Factor and Thermal Performance of an Artificially Broken Arc Rib Solar Air Heater. International Journal of Computational Materials Science and Engineering.

[24] Voisin,, Claire. (2023). Computational Analysis of Single-Pass Roughened Solar Air Heater Using Design of Experiment Approach. Advances in intelligent systems and computing, doi: 10.1007/978-981-19-9906-2_31

[25] N., Dilipsharma., Nicole, Raley, Vadivel., K., P., Ramesh., D., Kulandaivel., M., S., Babu. (2023). Analysis of Artificially Roughened Solar Air Heater Duct Using Computational Fluid Dynamics. International Journal For Science Technology And Engineering, doi: 10.22214/ijraset.2023.48751

[26] Ahmad, Abu-Akel. (2023). CFD-Based Performance Investigation of Convex Protrusion Shape Roughened Solar Air Heater. doi: 10.1007/978-981-19-6945-4_14

[27] Numerical investigation of fluid flow and heat characteristics of a roughened solar air heater with novel V-shaped ribs. Transactions of The Canadian Society for Mechanical Engineering, doi: 10.1139/tcsme-2021-0205
[28] Mebratu, Assaye., Muluken, Biadgelegn., Birlie, Fekadu. (2022). Numerical investigation of convection heat transfer in solar air heater with semi-circular shape transverse rib. Cogent engineering, doi: 10.1080/23311916.2022.2106930
[29] Analytical Study of Energy, Exergy and Thermohydraulic Performance Enhancement of Sustainable Solar Air Heater with C-Shape roughness. doi: 10.21203/rs.3.rs-2245980/v1
[30] Arin, Mishra., Aman, Mehrotra., S., Senthur, Prabu. (2022). Study on Performance Analysis of a Solar Air Heater with Aerofoil Shaped Rib Roughness Using CFD. ECS transactions, doi: 10.1149/10701.16065ecst
[31] Taler, D. (2005). Prediction of heat transfer correlations for compact heat exchangers. Forschung im Ingenieurwesen, 69(3), 137-150.